JOURNAL OF AIRCRAFT
Vol. 44, No. 4, July–August 2007

Response Surface Methods for Efficient Complex Aircraft Configuration Aerodynamic Characterization

Drew Landman*
Old Dominion University, Norfolk, Virginia 23529
Jim Simpson†
Florida State University, Tallahassee, Florida 32310
and
Dan Vicroy‡ and Peter Parker§
NASA Langley Research Center, Hampton, Virginia 23681

DOI: 10.2514/1.24810

A response surface methodology approach to wind-tunnel testing of aircraft with complex configurations is being investigated at the Langley full-scale tunnel as part of a series of tests using design of experiments. An exploratory study was conducted using response surface methodology and a 5% scale blended-wing-body model in an effort to efficiently characterize aerodynamic behavior as a function of attitude and multiple control surface inputs. This paper provides a direct comparison of the design of experiments/response surface methodology and one factor at a time methods for a low-speed wind-tunnel test of a blended-wing-body aircraft configuration with 11 actuated control surfaces. A modified fractional factorial design, augmented with center points and axial points, produced regression models for the characteristic aerodynamic forces and moments over a representative design space as a function of model attitude and control surface inputs. Model adequacy and uncertainty levels were described using robust statistical methods inherent to the response surface methodology practice. Experimental goals included the capture of fundamental stability and control data for simulation models and comparisons to baseline data from recent one factor at a time tests. Optimization is demonstrated for control surface allocation for a desired response. A discussion of highlights and problems associated with the test is included.

Nomenclature

C_A	=	axial force coefficient
C_l	=	rolling moment coefficient
C_m	=	pitching moment coefficient
C_N	=	normal force coefficient
C_n	=	yawing moment coefficient
C_y	=	side force coefficient
α	=	angle of attack in degrees, factor A
β	=	sideslip angle in degrees, factor B
δ_{Lrud}	=	left winglet rudder deflection in degrees, factor H, positive trailing edge left
δ_{L25}	=	left wing 2–5 ganged elevon deflection in degrees, factor E, positive trailing edge down
δ_{L67}	=	left wing 6–7 ganged lower elevon deflection in degrees, factor F, positive trailing edge down
δ_{L89}	=	left wing 8–9 ganged upper elevon deflection in degrees, factor G, positive trailing edge down
δ_{R25}	=	right wing 2–5 ganged elevon deflection in degrees, factor C, positive trailing edge down
δ_1	=	ganged left and right elevon 1 deflection in degrees, factor D, positive trailing edge down

Presented as Paper 0922 at the 2006 AIAA Aerospace Sciences, Reno, NV, 9–13 January 2006; received 25 April 2006; revision received 16 April 2007; accepted for publication 16 April 2007.

*Associate Professor, Department of Aerospace Engineering, 3750 Elkhorn Avenue, Suite 1300. Senior Member AIAA.
†Associate Professor, Department of Industrial Engineering, 2525 Pottsdamer Street. Member AIAA.
‡Senior Research Engineer, Flight Dynamics Branch, MS 308. Associate Fellow AIAA.
§Research Scientist, Aeronautics Systems Engineering Branch, MS 238. Member AIAA.

I. Introduction

THE process of wind-tunnel testing aircraft has the overall objective of characterizing aerodynamic stability, control, and performance. Changes are made to independent variables (factors) such as angle of attack, sideslip angle, and control surface deflections while the six aerodynamic force and moment responses are recorded. The traditional approach to testing is to vary one factor at a time (OFAT), holding all other factors as "constant." Researchers will then pursue a course of experimentation aimed at sequentially modifying other variables to obtain a mapping of the aerodynamic characteristics of interest. This approach requires that the entire system, which consists of the wind tunnel, the aircraft balance, and the data acquisition system, be completely stable throughout the entire test entry which may last several weeks. Any errors that result from variations in the system are confounded with precision errors and are inseparable. In addition, if two or more inputs interact to affect a response, the OFAT experimentation approach will not easily detect these important contributions to response prediction and system understanding.

Design of experiment (DOE) methods [of which response surface methodology (RSM) is a subset] approach an experiment by identifying all desired factors (independent variables) and all desired responses (outputs). Once all factors and responses are identified, a randomized run schedule is formulated that provides statistically based mathematical models of the responses in terms of the factors. The objective is to characterize the relationship between changes in system performance measures due to corresponding changes in system input factors. Bias errors due to uncontrolled or unknown system variations may be guarded against and uncertainty levels may be accurately estimated. Inherent to the DOE methodology is the construction of mathematical models detailing the response behavior being studied, capable of predicting performance measures over the factor design space studied.

Wind-tunnel testing often presents constraints to designs that are the staple of traditional industrial experimentation. In this study several control surface input factor settings were limited by interference with one another, requiring a departure from established

RSM designs. Automated control surfaces are well suited to a fully randomized test program but are nearly always a source of increased set point error when compared to a "fixed bracket" style surface setting. The RSM model presented here had to be robust to these potential sources of error. This study focused on proving test methods and is not an all-inclusive aerodynamic characterization of the chosen aircraft. The overall goal of the study presented here is to provide an efficient method of data collection for modeling and for aircraft aerodynamic database and simulation development.

II. Aircraft Configuration and Wind-Tunnel Model Design

The aircraft configuration used in this study was a trijet blended-wing-body (BWB) concept developed by the Boeing Company. The BWB concept evolved though a series of NASA funded design studies conducted by the McDonnell Douglas Company during the early 1990s [1]. The concept has shown potential for improved efficiency over the classic tube and wing configuration with reductions in both takeoff weight and fuel burn [2]. The Boeing Company developed this BWB configuration (BWB-450L) following their merger with the McDonnell Douglas Corporation in 1997. This design is the property of the Boeing Company and as such the geometry definition cannot be released without the permission of the Boeing Company. A three-view of the 5% scale model used in this study is shown in Fig. 1. The model has three pylon-mounted nacelles located on the upper surface of the aft centerbody. Each nacelle housed a pneumatic ejector connected to a high-pressure air supply to provide simulated thrust. The center nacelle could also rotate ±8 deg about the vertical body axis to simulate directional thrust vectoring. The control surfaces consist of 18 elevons distributed along the trailing edge, rudders on each winglet, and leading edge slats, as shown in Fig. 2. The two outboard elevons (labeled as "8 upper/6 lower" and "9 upper/7 lower") split to serve as both elevons and drag rudders. Because of weight constraints the model was limited to 11 actuators. This required several of the control surfaces to be ganged to a single actuator so they move in unison as if they were a single combined surface. This was the case with elevons 2–5, the upper elevons 8 and 9, and the lower elevons 6 and 7.

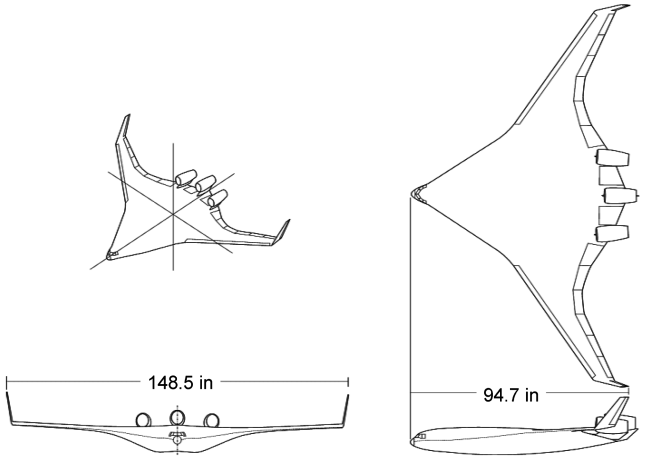

Fig. 1 5% model of blended wing body.

III. Static Testing Experiment Details

The test was conducted in two phases. The first phase used the classical OFAT approach over an angle-of-attack range from −10–30 deg and ±10 deg of sideslip. The second phase was exploratory in nature and employed a DOE/RSM approach over a limited angle-of-attack range from 5 to 10 deg and ±5 deg of sideslip. Comparisons of the two methods were conducted over this limited angle-of-attack and sideslip range. This wind-tunnel model was designed for a subsequent follow-on free-flight test in the same facility and was consequently equipped with remotely controlled actuators to drive the control surfaces. The remotely actuated surface capability made this test an ideal candidate for using a DOE/RSM approach. The objectives of the overall static test program were to measure the basic aerodynamics and control derivatives of the model, measure the thrust effects, and measure the effect of an attached cable in the free-flight test (umbilical cable).

A. RSM Experiment Objectives

Because the current study was part of a larger OFAT study, comparisons between the two approaches could be fairly judged. In addition previous data were available. The goals of this exploratory experiment can be summarized as follows.

1) Prove the feasibility of an RSM approach to rapidly gather an aerodynamic stability and control data set suitable for use in flight simulation software.

2) Compare the RSM approach to traditional methods in terms of resources required, resulting math models, response uncertainty, and value added.

3) Explore the utility of numerical optimization routines for control surface allocation.

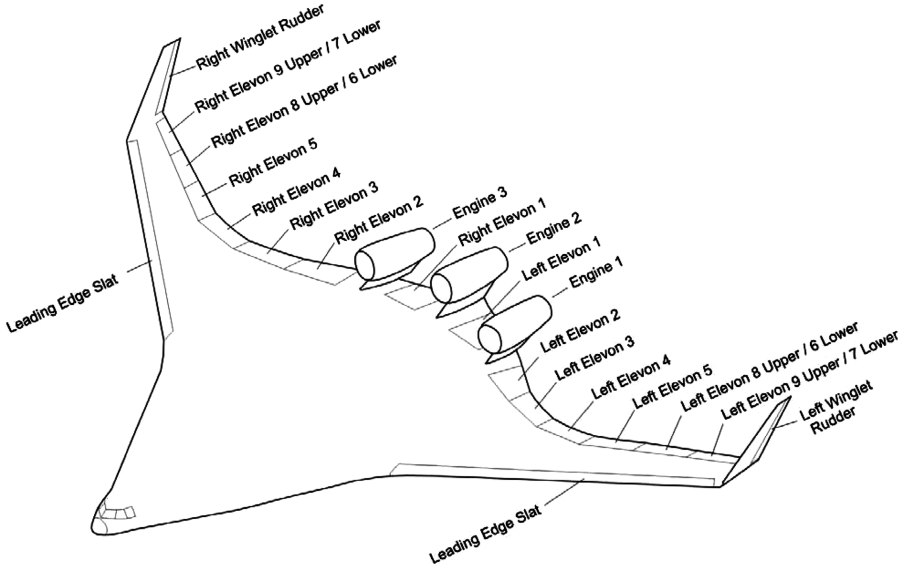

Fig. 2 BWB configuration control surfaces.

B. Facility

Old Dominion University, working under a memorandum of agreement with NASA Langley Research Center, operates the Langley full-scale tunnel (LFST). The open-jet test section is semi-elliptical in cross section with a width of 18.29 m (60 ft) and a height of 9.14 m (30 ft). The ground board is 13 m (42.5 ft) wide by 16 m (52.3 ft) long and features a turntable with a diameter of 8.7 m (28.5 ft). Power is supplied by two 3 MW (4000 hp) electric motors driving two 11 m (36 ft) diameter four-bladed wooden fans. The current maximum speed is limited to 210 rpm, which is about 130 kph (~80 mph) in the test section [3].

C. Model Mounting and Data Acquisition

The model support system used in this experiment consists of a large T structure with a long rear-entry sting and is shown in Fig. 3. Pitch setting is accomplished by articulation of the sting about the horizontal member. The entire T structure is rotated by the turntable to achieve sideslip settings. The dynamic pressure for the RSM test was nominally 383 Pa (8 psf).

The model forces and moments were measured with an internal six-component strain gauge balance sampled at 10 Hz. The measurements were averaged over a 20 s sample period for each data point. The accuracy of the balance at a nominal dynamic pressure of 383 Pa (8 psf) is given in Table 1. Corrections for flow angularity were applied to the data and obtained by a flow survey of the test section with a spatial resolution of 0.915 m (3 ft) [4].

Table 1 Internal strain gage balance uncertainties at test dynamic pressure of 8 psf

Response	95% confidence half-interval
C_A	0.00115
C_y	0.0018
C_N	0.00252
C_l	0.00006
C_m	0.00012
C_n	0.00007

IV. Use of Design of Experiments

The formal design of experiments in its broadest sense is a process for planning an experiment so that appropriate data can be collected and analyzed by statistical methods, resulting in valid and objective conclusions [5,6]. A test matrix benefits from the three basic tenets of DOE: replication, randomization, and blocking. Randomization is the cornerstone of statistical methods in experimental design and requires that both the experimental factor choices and the order of the runs are randomly determined. Randomization also assists in averaging out the effects of extraneous factors that may be present. Replication is the repetition of runs within the basic experiment. Replication of design points allows the researcher to determine an internal estimate of system noise and uncertainty. Blocking is a technique used to improve the precision with which comparisons among the factors of interests are made. Blocking is also used for reducing the variability transmitted through nuisance factors, that is, factors that may influence the experimental response but that are of no direct interest. For example, variations in wind-tunnel measurements are often encountered when comparing overnight runs or shifts. Assigning groups of runs to blocks helps separate the shift-to-shift variability due to atmospheric conditions or personnel changes, or from changes in the force balance precision. RSM is a refinement to DOE and poses three general objectives in industrial experimentation: mapping a response surface over a particular region of interest, optimization of the responses, and selection of operating conditions to achieve specifications or customer requirements [7].

Analysis of the experimental data is performed using statistical hypothesis testing and regression model building so that the response values can be accurately estimated or predicted using empirical models. These models are usually low-order polynomial functions of the input variables (factors) but, with enough degrees of freedom in the test matrix, can be of higher order. The model is also tested for adequacy relative to fitting data (lack-of-fit test). One of the greatest benefits in using DOE/RSM methods versus the traditional OFAT methods is the ability to include interaction terms in the analysis. The OFAT method allows only for one variable to be changed at a time, therefore it typically evaluates main effects. The DOE/RSM method allows, and partially requires, the change of more than one factor simultaneously, thus allowing for the discovery of interaction between variables. For example, OFAT testing can easily find the effect of the deflection of a trailing edge control surface on pitching moment over a yaw sweep. DOE testing can efficiently identify any and all interaction effects on pitching moment, between any or all deflected control surfaces, over any yaw angle within the design space. The relative magnitudes of the model coefficients give direct feedback as to the importance of the interaction effects to the prediction of the responses.

Model design using a classical sequential DOE approach typically starts by allocating a subset of design points for building a linear model based on two-level factor settings. These factorial based models are then tested for fit and if found inadequate are augmented with additional points, yielding a quadratic model. Classical RSM second-order designs focus on optimizing the design matrix for prediction variance and avoiding correlation over spherical or cuboidal experimental design spaces. If higher-order models are necessary, second-order designs can be augmented with additional test points to fit the high-order terms.

The advantage to using designed experiments in wind-tunnel testing has been explored in recent years and is gaining in popularity [8–11]. The objective of this paper is to try and add to the growing number of case studies and not to provide a comprehensive treatise on the use of designed experiments.

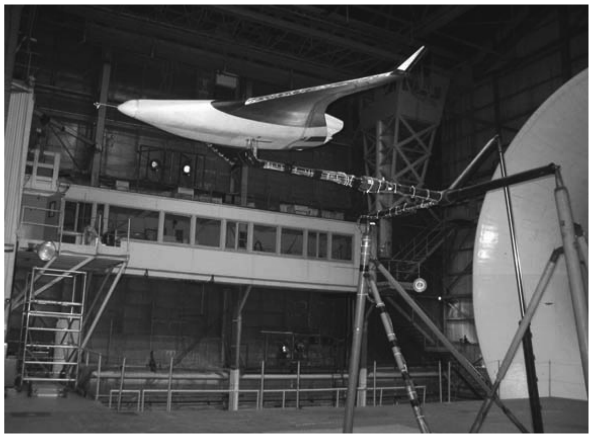

Fig. 3 BWB model mounted in Langley full-scale tunnel.

V. Experiment Design

A. Factor Choices and Constraints

Resources for this exploratory project were limited so that a subset of representative factors was chosen. Angle of attack and sideslip angle were of course required factors for longitudinal and lateral aerodynamic characterization. Interest focused on possible interactions between control surfaces with particular regard to those located adjacent to each other. It was decided to choose the left (port) trailing edge elevons and winglet rudder and to include right influences using the right 2–5 ganged elevons. A mechanical constraint is present due to the collocation of lower surfaces 6–7 and upper surfaces 8–9. These can be deployed as drag rudders with 8–9 deflected up and 6–7 deflected down or as elevons with both deflected in the same direction. The deflection constraint which arises from their actuation limits and interference is given as $\delta_{L67}-\delta_{L89} > 5$ deg.

The range of angle of attack was chosen so as to bracket the cruise condition and avoid stall, and a small sideslip range was chosen to provide yaw sensitivity. Control surface limits were chosen to cover

Table 2 Factor levels and constraints

Factor	Factor ID	Low	Center	High	Constraints
α	A	4	7	10	None
β	B	−5	0	5	None
δ_{R25}	C	−30	−5	20	None
δ_{1}	D	−30	−5	20	None
δ_{L25}	E	−30	−5	20	None
δ_{L67}	F	−30	10	50	F − G > 5
δ_{L89}	G	−50	−15	20	F − G > 5
δ_{Lrud}	H	−20	5	30	None

the full designed deflection range. However, in practice mechanical limits of the model limited the deflection of elevons 8–9 and 6–7 to less than their design limits. The eight factors, their nominal design levels, and constraints are summarized in Table 2.

B. Traditional Augmented Factorial Model Design

Two-level factorial designs are foundational to designed experiments because they provide an efficient experimental strategy to explore first-order effects and two-factor interactions. In these designs, the factors of interest are changed between predetermined high and low levels, often denoted in coded units as the +1 and −1 levels. The first step to building a design requires the experimenter to identify the *region of interest* and the *region of operability*. The region of interest defines the upper and lower limits of the factor settings in which an empirical model is desired, whereas the region of operability is defined by the upper (+1 level) and lower (−1 level) limits of the factor settings that can be achieved safely. In the current study, these regions are coincident and using a two-level factorial design results in a cuboidal design space, referred to as a hypercuboidal region in eight-dimensional space. Augmenting a two-level factorial design with center points (design points taken at the center of each factor range) allows for the detection of curvature, which may indicate that a first-order plus two-factor interaction model is not sufficient in capturing the factor-response relationship. Furthermore, the center points are replicated to provide an internal estimate of the experimental error, the inherent process variability or process noise, allowing for a determination of individual factor effect significance aiding in the construction of parsimonious models [5,6].

If curvature is detected, then the design can be further augmented with design points, known as axial points, which together with the factorial and center points support the estimation of a complete second-order model. The resulting design is a classic central composite design (CCD) and is classified by the distance from the design center to the axial points [7]. The term axial indicates that these design points lie on the factor axes of the design space, denoting that all other factor levels are set to zero. Two axial points are added for each factor. In this experiment, a distance of one was employed resulting in a face-centered CCD (FCD). A distance of one maintains the convenience of only three discrete level settings for each factor.

Employing a full two-level factorial design in eight factors results in $2^8 = 256$ design combinations. This design supports the estimation of all main effects, and all multiway interactions up to and including a single eight-factor interaction. Making the assumption that many higher-order interactions are not necessary to estimate an adequate empirical model allows the full two-level factorial to be fractionated, resulting in fewer experimental runs. In this study, a $\frac{1}{2}$ fraction was generated, known as a $2^{(8-1)}$, requiring 128 runs. The fractionation is performed in a manner that retains the ability to uniquely estimate the maximum number of lower-order effects, a concept known as minimum aberration. In a sense, a minimum aberration design minimizes the impact of the reduced information obtained from the fractionation as compared to executing the full factorial. The resulting 128-run fractional design supports the unique estimation of all main effects, two-factor, and three-factor interactions assuming that four-way and higher interactions are negligible.

C. Final Model Design

To accommodate the particular mechanical constraints due to the test article configuration, the fractional factorial design was modified manually resulting in an asymmetric design space. The constraint and subsequent model modification are shown in two-dimensional space in Fig. 4. Here the two affected factors are first shown in an unconstrained FCD. Applying the constraint results in a clipping of the top left corner of the square so as to move the top left factorial point and the upper face-centered axial to the right. As a result, the orthogonality of the design was disrupted producing overlapping information when estimating the factor effects. Collinearity refers to the amount of overlap and can be quantified by computing the variance inflation factor (VIF) for each model term. In general, a VIF of less than 10 is desirable, which was achieved in the modified design [7]. In this case, modifying a classical design was successful because the constraints were not too severe. Consequently, many of the desirable properties of the classical design were retained. Before the test the constrained FCD model was evaluated using a BWB flight simulation model developed from previous testing [12].

To summarize, the experimental design to study the eight constrained factors is based on a 128 run fractional factorial combined with 16 face-centered axial points and features eight replicated center points, requiring a total of 152 runs. The design was conducted in two blocks, the first with the 128 factorial combinations and four centers, and the second with the 16 axial points and four centers. For brevity, the full design is not included in this report. This final design represents an efficient strategy to estimate the 45 terms in a full second-order model in eight factors. Moreover, it provides sufficient degrees of freedom to estimate the experimental error allowing for an objective assessment of the adequacy of a second-order model.

VI. Results and Discussion

A. Analysis of Results

The data collected were analyzed using least squares estimation with the aid of Design Expert™, a commercially available program. First, a tentative regression model with all factors was developed for each of the responses up to and including three factor interactions. The purpose of this analysis is to determine which factors, multifactor interactions, and higher-order polynomial terms affect each response to develop an empirical model that accurately predicts response values for any factor settings between the low and the high levels. Using the mean squares for each model term versus the mean square for error, an F test is performed to determine statistical significance. The model is consequently refined by dropping insignificant terms and a table of significance, called the analysis of variance (ANOVA) table, is then computed. An example for the axial response is shown in Table 3. The model is considered tentative until the model assumptions of normally, independently distributed errors with constant variance are tested. The model residuals, the difference between model response values and the regression model predicted response values, are estimates of the true model errors. Normality is evaluated by plotting rank-ordered observations against their observed cumulative frequency and is somewhat subjective. No problems were encountered with normality in this study, however, the level of noise was significant. Plotting residuals versus predicted values provides a check for constant variance, a fundamental requirement to the model fitting. Finally, plotting residuals versus

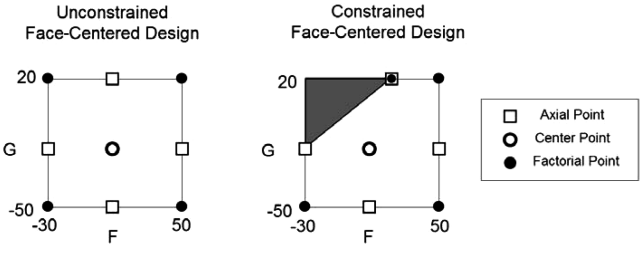

Fig. 4 Face-centered design modifications.

Table 3 Example ANOVA table

ANOVA for axial force coefficient response surface					
Source	Sum of squares	DF	Mean square	F value	Prob > F
Block	0.005985	1	0.005984528	——	——
Model	0.229783	24	0.009574301	4653.35	<0.0001
A	0.173022	1	0.173022038	84092.96	<0.0001
B	2.06E-05	1	2.06319E-05	10.03	0.0019
C	0.019821	1	0.019820604	9633.30	<0.0001
D	0.004135	1	0.00413513	2009.77	<0.0001
E	0.020453	1	0.02045337	9940.84	<0.0001
G	0.001459	1	0.001458836	709.03	<0.0001
H	5.44E-05	1	5.43938E-05	26.44	<0.0001
A^2	0.000104	1	0.000104421	50.75	<0.0001
C^2	7.5E-05	1	7.50489E-05	36.48	<0.0001
D^2	0.00018	1	0.000179928	87.45	<0.0001
E^2	0.000168	1	0.000167511	81.41	<0.0001
G^2	1.47E-05	1	1.4661E-05	7.13	0.0086
AC	0.000714	1	0.000713931	346.99	<0.0001
AD	4.07E-05	1	4.07467E-05	19.80	<0.0001
AE	0.000587	1	0.000586571	285.09	<0.0001
AG	9.73E-06	1	9.7253E-06	4.73	0.0315
BC	9.7E-06	1	9.69944E-06	4.71	0.0318
BD	8.14E-06	1	8.13558E-06	3.95	0.0489
BE	9.6E-06	1	9.60243E-06	4.67	0.0326
BG	8.69E-06	1	8.69074E-06	4.22	0.0419
CD	2.21E-05	1	2.2106E-05	10.74	0.0013
CE	0.000195	1	0.000194804	94.68	<0.0001
CG	1.67E-05	1	1.67106E-05	8.12	0.0051
DE	4.18E-05	1	4.18403E-05	20.34	<0.0001
Residual	0.000263	128	2.05751E-06	——	——
Cor. total	0.236031	153	——	——	——

run checks for systematic variation over time that may mean the assumption of independence has been violated. No structure in the residuals should be observed and they should remain within an upper and lower limit of 3 standard deviation units. No anomalies were found other than a larger than expected noise level as shown in the example of Fig. 5. For the sake of brevity all remaining diagnostic plots were omitted from this publication. Having passed the diagnostic checks, a regression model for each of the aerodynamic coefficient responses was now available. Note that the term definitions are given under the nomenclature section and that model hierarchy was maintained. A 95% confidence half-interval on the response is computed by taking 2 times the square root of the mean square for error (shown under the heading of "residual" in the example of Table 3). Uncertainty values are presented in Table 4 for each of the responses and include all control surface set point errors, force balance precision, and associated data acquisition system uncertainty.

B. Comparisons to OFAT Data

Direct comparisons between OFAT and RSM responses are presented in Table 4. Average differences between existing OFAT data points and RSM model predicted values are shown to lie well within the confidence intervals established by the uncertainty estimates from the RSM study. As a graphical example consider the pitching moment and normal force response surfaces as a function of angle of attack and deflection of the left ganged elevon 2–5 shown in

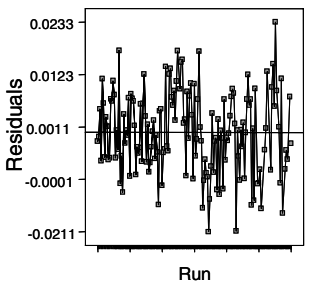

Fig. 5 Residuals of C_N response.

Table 4 Comparisons of average response differences and uncertainty levels

Response	95% confidence interval	Average difference RSM–OFAT
C_A	0.0057	0.0011
C_y	0.0073	0.0028
C_N	0.0365	−0.0291
C_l	0.0066	0.0020
C_m	0.0069	0.0062
C_n	0.0015	0.0000

Figs. 6 and 7. As noted in Table 4 and shown in Fig. 6 the RSM normal force predicted values were on average less than the OFAT data. Figure 7 shows that the corresponding RSM pitching moment values were on average greater than the OFAT data points. These differences may be due to system variances that are not accounted for in the OFAT approach. Comparison of the number of data points used with the two test methods illustrates the primary difference in these approaches. The OFAT test matrix, which was designed to provide a desired data density, resulted in 287 points in the same design space as the DOE/RSM covered with 128 points. The OFAT desired data density for stability and control characterization is chosen with increments of every 2–4 deg angle of attack in the linear lift region and every 1 or 0.5 deg in the nonlinear regions of lift, drag, or pitching moment. This data density requirement is empirically based on minimizing the interpolation error between data points. The DOE/RSM test matrix, which was designed to provide a desired model also provides multiple-factor interactions not directly available from the OFAT data.

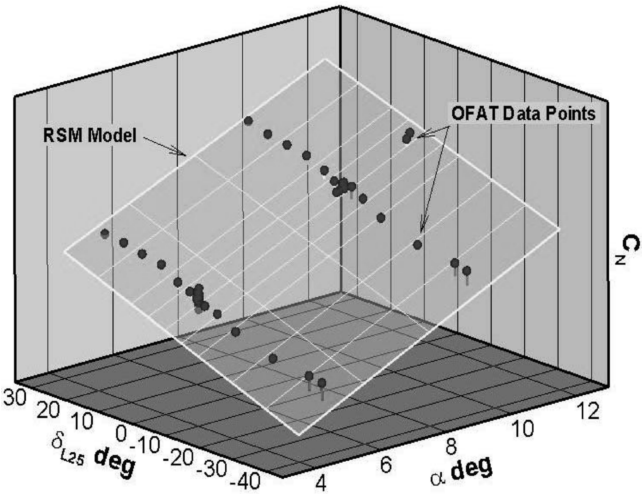

Fig. 6 RSM to OFAT comparison, C_N.

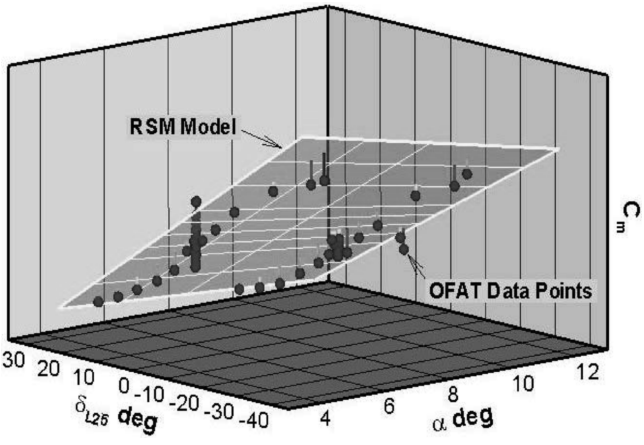

Fig. 7 RSM to OFAT comparison, C_m.

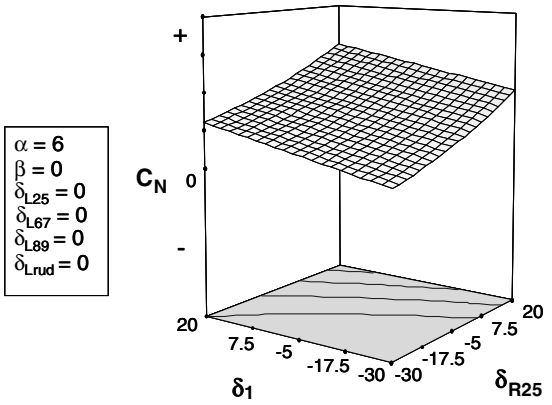

Fig. 8 Control surface interaction: C_N.

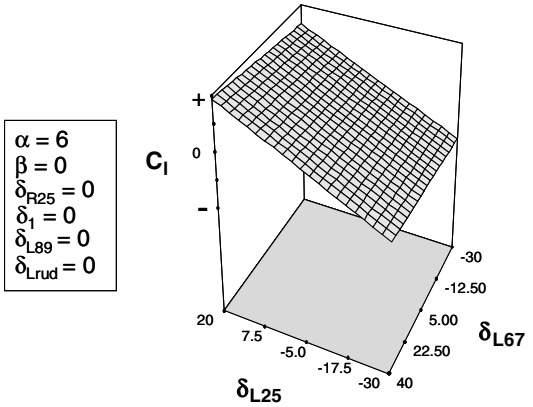

Fig. 9 Control surface interaction: C_l.

C. Interactions and Optimization

An interaction occurs when one factor produces an effect on the response that is dependent on the setting of another factor. In this study, interest focused on the probable synergistic behavior of adjoining trailing edge control surfaces. An example is seen in the normal force response to δ_{R25} and δ_1 shown in Fig. 8. This interaction plot shows that the normal force due to deflecting both surfaces is greater than the sum of either surface deflected alone. As a second example consider the rolling moment response (Fig. 9) due to δ_{L25} and δ_{67}. Again the sum of the individual responses is less than their combined effect. Although this is not surprising perhaps, it is identified directly and quantified with the RSM methodology.

Aircraft with complex control surface configurations present an interesting opportunity in that choices arise in the allocation of surfaces to achieve specific control objectives. The RSM model inherently includes all the effects of all surface deflections for any response, ideal for optimization routines. As an example, consider the yawing moment response for this flying wing design. The interaction plot for the port wing split surfaces is shown in Fig. 10 including the excluded response area resulting from the constraint. An example of multiple response constrained optimization was generated using a desirability approach to maximize yawing moment response while minimizing roll moment response [13]. Equally weighted goals are presented in Table 5 where it should be noted that the yawing moment is minimized due to the desire to achieve the most negative value. In this example the attitude, starboard control surfaces, and body elevon are fixed and the port control surfaces are unconstrained. Results are presented as Table 6 where the best solution is given by the highest desirability rating. The split surfaces (drag rudder) are seen to be deflected for maximum drag and the rudder for maximum yaw (magnitude) where the ganged 2–5 surfaces are used to "trim" for minimum roll.

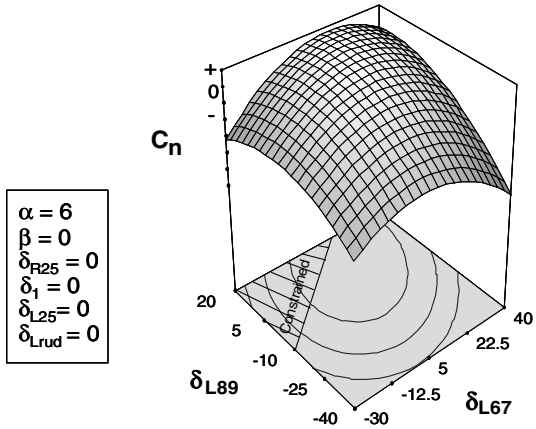

Fig. 10 Yawing moment response.

D. Lessons Learned

The modified FCD specified control surface set points were different in practice than in the design. Issues arose with actuator positioning as well as manufacturing tolerances in control surface fits. Post test analysis discovered that control surface potentiometer readings showed that surface position had a relatively high variance leading to the high estimates of uncertainty that have been presented. Although neither of these problems is desirable, they did serve to test the overall effectiveness of the RSM method in the presence of higher than expected noise and further promote the use of methods that inherently identify the overall uncertainty in an environment with many variables both known and lurking (unknown).

Table 5 Optimization constraints to maximize yaw moment response with minimum roll

Name	Goal	Lower limit	Upper limit
α	Is equal to 6.00	5.1	11.4
β	Is equal to 0.00	−5	5
δ_{R25}	Is equal to 0.00	−30	20
δ_1	Is equal to 0.00	−30	20
δ_{L25}	Is in range	−30	20
δ_{L67}	Is in range	−30	40
δ_{L89}	Is in range	−35.85	19.2
δ_{Lrud}	Is in range	−20	30
C_l	Is target = 0	——	——
C_n	Minimize	——	——

Table 6 Optimizer solutions

Solution	δ_{L25}	δ_{L67}	δ_{L89}	δ_{Lrud}	C_n, % best	C_l/C_n, %	Desirability
1	−6.44	40.00	−33.98	30.00	90.11	0.842	0.823
2	−11.54	40.00	−35.85	30.00	100.00	80.686	0.806
3	−10.10	40.00	−13.39	29.93	73.61	0.000	0.789
4	2.69	−26.45	−35.83	30.00	71.63	0.001	0.785
5	2.50	−25.08	−35.85	29.97	70.61	0.188	0.783
6	−3.22	17.80	−35.85	30.00	69.77	−0.003	0.781
7	1.45	−17.31	−35.85	29.88	65.91	−0.003	0.773

VII. Conclusions

The modified face-centered design proved effective at characterizing the aerodynamic behavior of the BWB for the subset of factors chosen. The approach was robust to the unexpectedly high noise levels attributed primarily to the control surface set point error. Complex configurations can benefit greatly from response surface methods in that a mathematical model for aerodynamic characterization is developed with minimum required runs and is well suited for optimization.

References

[1] Liebeck, R., "Blended-Wing-Body Technology Study," Final Report, NASA Contract NAS1-20275, Boeing Report CRAD-9405-TR-3780, Oct. 1997.

[2] Liebeck, R., "Design of the Blended-Wing-Body Subsonic Transport," AIAA Paper 2002-0002, 2002.

[3] Britcher, C. P., and Landman, D., "From the 30×60 to the Langley Full-Scale Tunnel," AIAA Paper 1998-0145, 1998.

[4] Alvarez, J., and Landman, D., "Test Section Flow Quality Surveys of the Langley Full-Scale Tunnel," AIAA Paper 2002-0739, 2002.

[5] Montgomery, D. C., *Design and Analysis of Experiments*, 6th ed., Wiley, New York, 2004.

[6] Box, G. E. P., Hunter, J. S., and Hunter, W. G., *Statistics for Experimenters: Design, Innovation and Discovery*, 2nd ed., Wiley, New York, 2005.

[7] Myers, R. H., and Montgomery, D. C., *Response Surface Methodology*, 2nd ed., Wiley, New York, 2002.

[8] DeLoach, R., "Tactical Defenses Against Systematic Variation in Wind Tunnel Testing," AIAA Paper 2002-0885, 2002.

[9] Landman, D., Simpson, J., Hall, B., and Sumner, T., "Use of Designed Experiments in Wind Tunnel Testing of Performance Automobiles," *SAE 2002 Transactions: Journal of Passenger Cars—Mechanical Systems*, 2002, pp. 2339–2346.

[10] DeLoach, R., and Berrier, B. L., "Productivity and Quality Enhancements in a Configuration Aerodynamics Test Using the Modern Design of Experiments," AIAA Paper 2004-1145, 2004.

[11] Landman, D., Simpson, J. R., Mariani, R., Ortiz, F., and Britcher, C., "A High Performance Aircraft Wind Tunnel Test Using Response Surface Methodologies," AIAA Paper 2005-7602, 2005.

[12] Vicroy, D., Murri, D., and Grafton, S., "Low-Speed, Large Angle Wind Tunnel Investigation of a Subsonic Blended-Wing-Body Tri-Jet Configuration," NASA CDTM-10044, 2004.

[13] Derringer, G., and Suich, R., "Simultaneous Optimization of Several Response Variables," *Journal of Quality Technology*, Vol. 12, Jan. 1980, pp. 214–219.